

The impact of a high-sodium diet regimen on cerebrovascular morphology and cerebral perfusion in Alzheimer's disease

Jin Yu^a, Hong Zhu^a, Mark S. Kindy^{a,c}, Saeid Taheri^{a,b,*}

^a Department of Pharmaceutical Sciences, University of South Florida, Tampa, FL 33612, USA

^b USF Heart Institute, Tampa, FL 33612, USA

^c James A. Haley VA Medical Center, Tampa, FL 33612, USA

ARTICLE INFO

Keywords:

Alzheimer's disease
Cerebrovascular circulation
Cerebrovascular density
Magnetic resonance imaging
Diffusion MRI

ABSTRACT

Introduction: Various lifestyle factors such as chronic hypertension and a high-sodium diet regimen are shown to impact cerebrovascular morphology and structure. Unusual cerebrovascular morphological and structural changes may contribute to cerebral hypoperfusion in Alzheimer's disease (AD). The objective of this study was to examine whether a high-sodium diet mediates cerebrovascular morphology and cerebral perfusion alterations in AD.

Methods: Double transgenic mice harboring A β precursor protein (APP^{swe}) and presenilin-1 (PSEN1) along with wild-type controls were divided into four groups. Group A (APP/PS1) and B (controls) were both fed a high-sodium (4.00%), while group C (APP/PS1) and D (controls) were both fed a low-sodium (0.08% a regular chow diet) for three months. Then, changes in regional cerebral perfusion and diffusion, cerebrovascular morphology, and structure were quantified.

Results: A 3-month high-sodium diet causes pyknosis and deep staining in hippocampal neurons and reduced vascular density in both hippocampal and cortical areas ($p < 0.001$) of APP/PS1. Despite vascular density changes, cerebral perfusion was not increased markedly ($p = 0.3$) in this group, though it was increased more in wild-type controls ($p = 0.022$).

Conclusion: A high-sodium diet regimen causes cerebrovascular morphology alteration in APP/PS1 mouse model of AD.

1. Introduction

Associated with cerebral hypoperfusion, impaired cerebrovascular (CV) functions such as reactivity and resistance index are frequently observed in Alzheimer's disease (AD) patients [1,2]. A wide range of pathologies, such as arterial stiffness and capillary reactivity dysfunction, have been shown to contribute to CV dysfunction [1,3]. Both animal models of AD and patients with AD have shown structural changes to their cerebral vessels, including decreased microvascular density and shrinkage of vessel diameter [4,5]. However, even in the absence of a background cerebrovascular pathology, various lifestyle factors, including chronically high mean arterial pressure (MAP) and a high-sodium diet are found to influence cerebrovascular morphology and structure.

The presence of chronic high MAP is one of the systemic anomalies

that is often associated with structural changes in the small vessels in the brain [6]. According to research, this is attributed to a reduced cerebral blood flow (CBF) and a reduced lower limit of the CBF autoregulation mechanism [7–10]. There is a correlation between impaired CBF autoregulation and abnormal A β accumulation in patients with cognitive impairments and AD [11,12]. Chronic high MAP may contribute to AD pathology through both altered vascular function and morphology [13,14]. It is imperative to note that chronic high MAP is linked to AD neurodegeneration through several non-vascular mechanisms, particularly in the hippocampus [15–17]. For example, experimental studies support the synergistic effects of chronic high MAP and aging on the expression of genes involved in the A β generation in AD [18].

Multiple factors, alone or in synergy, may contribute to the pathogenesis of chronic high MAP [19]. Excess dietary salt intake is the most significant controllable factor responsible for the rise in MAP with

* Corresponding author at: Department of Pharmaceutical Sciences, USF Heart Institute, University of South Florida, 12901 Bruce B. Downs Blvd., MDC 30, Tampa, FL 33612, USA.

E-mail address: taheris@health.usf.edu (S. Taheri).

<https://doi.org/10.1016/j.cccb.2023.100161>

Received 19 May 2022; Received in revised form 5 December 2022; Accepted 27 January 2023

Available online 29 January 2023

2666-2450/© 2023 Published by Elsevier B.V. This is an open access article under the CC BY-NC-ND license (<http://creativecommons.org/licenses/by-nc-nd/4.0/>).

advancing age [20–22]. Interestingly, excess dietary salt intake has been shown to directly damage cerebrovascular elements, particularly endothelial cells [23–28]. An earlier study showed that a high-sodium diet regimen affected MAP and CBF differently in a transgenic mouse model of AD compared to a WTC [29]. However, the role of a high-sodium diet regimen in inducing high MAP and altering cerebral perfusion in AD is not clear. The purpose of this study was to use a mouse model of AD and test the hypothesis that a human lifestyle with a high-sodium diet regimen impacts CV morphology and structure, which may lead to cellular damage within brain regions which are crucial for memory and cognition.

A number of transgenic mouse models have been developed to simulate AD at the molecular level. APP/PS1 mice model of AD exhibit a remarkable elevation of β -amyloid production, which is accompanied by certain behavioral abnormalities [29]. Recent studies have shown that in APP/PS1, an A β plaque-generating mouse model, cerebral microcirculatory disturbances exist followed by increased reactive astrocytes and neurodegeneration [30,31]. In particular, the vessels in the cortex and hippocampus of APP/PS1 mice exhibit abnormal morphology [32]. While these results show the role of cerebrovascular disorders in AD, it remains unclear whether socio-behavioral factors, such as diet, have influenced cerebrovascular morphology and cerebral perfusion in the anatomical areas affected by AD.

This study contributes to the current literature by using advanced *in vivo* MR imaging techniques as well as experimental models that simulate a high-sodium diet lifestyle associated with AD. It is hypothesized that a high-sodium diet regimen alters cerebral perfusion through morphological changes in the cerebrovascular system. Additionally, we hypothesized that a high-sodium diet would alter cerebral perfusion in a mouse model of AD.

2. Materials and methods

2.1. Subjects

Double transgenic mice (2 X Tg-AD) harboring beta-amyloid precursor protein (APP^{swE}) and a mutant human presenilin-1 (PS1) were originally purchased from the Jackson Laboratory (MMRRC Stock No: 34,832-JAX, Bar Harbor, ME) and bred in the animal care facility at the University of South Florida (USF). Wild-type littermates were used as WTC (10–20 w, 25–30 g). Mice were group-housed (5 per cage) in a temperature- and humidity-controlled vivarium on a reversed 12:12 light-dark cycle. Mice received *ad libitum* food and water (Harlan, Indianapolis, IN, USA). All animal procedures were conducted in accordance with the “Guide for the Care and Use of Laboratory Animals” (Institute of Laboratory Animal Resources on Life Sciences, National Research Council, 1996) and approved by the IACUC of USF (IS00007666).

2.2. Genotyping

Standard genotyping protocols were followed to confirm the presence of APP^{swE}/PSEN1^{dE9} transgene in-house breed mice (see <http://jaxmice.jax.org/strain/005864>).

2.3. Experimental groups

APP/PS1 mice, along with wild-type controls (WTC), two months of age at initiation of special diet, were divided into four groups: Group A, APP/PS1, $n = 13$, and Group B, WTC, $n = 13$ both were fed a high-sodium (4.00%) chow diet for three months; Group C, APP/PS1, $n = 13$ and Group D, WTC, $n = 13$ both were fed a low-sodium (0.08% NaCl a regular chow diet) for three months.

2.4. Experiments timeline

Experiments were strictly randomized and blinded. The mice were weaned at 22 days after birth, fed a low-sodium diet for five weeks then fed either a low-sodium diet or a high-sodium diet for three months. At 70 days on the diet, blood pressure was measured three times each a week apart. Seven days after that, mice underwent MR imaging. At the end of the experiments, mice were euthanized and brains were harvested for histological analysis. WTC + APP/PS1 with high-sodium diet; $n = 10$; 21 ± 0.6 weeks; range 4 to 5 weeks (three attrition per group). WTC + APP/PS1 fed low-sodium diet $n = 10$; 21 ± 1.2 weeks; range 4 to 5 weeks (three attrition per group). The timeline of experiments and *in vivo* MR imaging sessions is depicted in Fig. 1.

2.5. Diet

Mice were fed a low-sodium (0.08% NaCl) or a high-sodium (4% NaCl) diet (Harlan Laboratories Inc. Indianapolis, IN- “TD09078”) for three months. A diet with 4% NaCl was implemented to induce experimental hypertension [33].

2.6. Blood pressure measurements

Conscious heart rate, systolic arterial blood pressure (SAP), and diastolic arterial blood pressure (DAP) were measured noninvasively at 20–22 weeks of age using a tail blood pressure volume measurement device (CODA system, Kent Scientific Corporation, Torrington, CT, USA) before the end of a three-month controlled diet (Fig. 1). The measurement protocol was described earlier [34,35]. In brief, mice were immobilized in plastic holders and acclimated to the restrainer for 10 min per day for at least three days before data collection. Then, alert unanesthetized mice were immobilized in plastic holders and allowed 10 min of acclimation before the tail-cuff measurements. Data on SAP, DAP, tail blood volume, and heart rate were collected. Data collection was done as the mean of two acclimation and 10 or 15 measurement cycles that took approximately 20 min.

2.7. Histological assessments

Mice were euthanized by exposure to a saturated atmosphere of isoflurane. Immediately after euthanasia, the brain was perfused with saline and 4% paraformaldehyde. The brain was removed and placed in 4% paraformaldehyde overnight. The brains fixed in 4% paraformaldehyde were processed and embedded in paraffin. Ten serial 30 μ m-thick sections through the brain were obtained using a microtome. Cryosections of the brain hemispheres were washed three times (5 min/wash) with Tris-buffered saline (TBS) (pH 7.4) buffer, followed by washing once with 0.1% Triton X-100-TBS buffer for 5 min. Sections were then incubated in 3% H₂O₂ and TBS buffer for 30 min at room temperature to eliminate endogenous peroxidase activity.

2.7.1. Morphometric measurements

The diameter of blood vessels was measured by type IV collagen immunoreactivity. From prepared brain tissue, 30- μ -thick sections were prepared for immunohistochemistry. Collagen IV (Chemicon, MilliporeSigma AB756P) was stained overnight; and tetramethyl rhodamine isothiocyanate (TRITC) goat antirabbit antibody was used as a secondary antibody. Three images per section were taken by light microscopy. Total vessel length and the length of segments covered by collagen IV were traced in three random regions (each region was 700 μ by 700 μ) for each 100 μ -thick section. On average, 50 vessel segments were measured per brain.

2.7.2. Cresyl violet Nissl staining

Paraformaldehyde-fixed tissue sections were assessed for gross neuronal damage with Cresyl Violet acetate standard staining

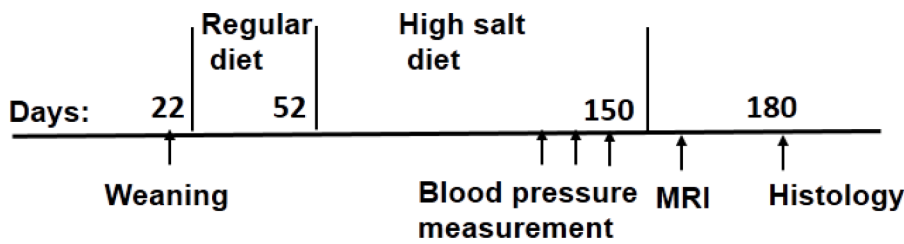


Fig. 1. Study design. Four randomized experimental groups of mice were designed to investigate the impact of a high-sodium diet on cerebral perfusion in the presence of accumulated Aβ. Mice weaned at 22 days after birth were used in the experiment. All mice were first fed a low-sodium diet for one month and then fed either a low-sodium or a high-sodium diet for three months. At 70 days on the diet, blood pressure was measured three times each a week apart. Seven days after that, mice underwent *in vivo* MR imaging. The high-sodium diet regimen lasted three months and

began about four weeks after weaning. Advanced *in vivo* MR diffusion and perfusion techniques were used to investigate cerebral perfusion and water diffusion. At the end of the experiment mice were euthanized and brains were harvested for histological analysis. Histological assessments were used to investigate cerebral vessels morphology and neuronal damage in areas critical to memory and cognition.

techniques. Briefly, fixed brain tissues were serially sectioned at 5 μm. Slides were rehydrated with decreased ethanol concentrations: 100% (three times), 95% (twice), 70%, and subsequently dipped for 10–20 min in 0.25% Cresyl violet (Sigma-Aldrich, Inc., USA). Slides were immersed shortly in PBS followed by fast wash in 25% ethanol, and differentiated in 50% ethanol + 0.5% acetic acid for about 3 min to reduce nonspecific and Glia staining. Counterstaining was performed followed by section dehydration in ascending series of ethanol, clearing with xylenes, and coverslipping with DPX (Sigma-Aldrich, Inc., USA). Images from Nissl stained and collagen IV stained sections were captured under an Olympus BX-51 bright field microscope equipped with an Optronics digital camera. Coronal sections (5 μm) within the coordinates of 2.46 mm interaural and –1.34mm bregma and 0.64 mm interaural and –3.16 mm bregma were selected for analysis. Coronal sections at 0.64 mm interaural and –3.16 mm bregma were selected for representation.

2.8. Blood vessel data analysis

Data labels were randomized and a blinded investigator (H.Z.) counted the number of unique blood vessel branches and measured blood vessels diameters in each binary image. Microscopic images were processed using ImageJ (NIH, V1.53 h) to highlight collagen IV stained vessels. Then we drew a line perpendicular to the long axis of each visible blood vessel to measure its diameter at its widest point following the full width at half-maximum algorithm [36]. The histograms of blood vessel diameters were generated for visual comparison using the R package (version 3.5.3, R Development Core Team 2020).

2.9. MR imaging

Imaging was performed on a 7T BioSpec research dedicated MR scanner (Bruker Biospin, Ettlingen, Germany), equipped with 500 mT/m (rise time 80–120μs) gradient set (for performing high resolution small animal imaging) and a small bore linear radio frequency (RF) coil (ID 119 mm) as the RF transmitter and a four channel surface array coil as the RF receiver. Mice were anesthetized using isoflurane gas (induction dosage 1–1.5%, maintenance dosage 0.5%–1%), at 1 L/min N₂O/O₂ (70/30) flow under spontaneous respiration, during which we collected data. Physiological parameters (heart rate, respiratory rate, and body temperature) were monitored during the imaging session for signs of distress and to ensure normal physiological parameters using SAI monitoring instruments (Small Animal Instruments Inc., Stony Brook, NY). A controlled warm airflow is kept in place inside the magnet to maintain the body’s core temperature.

The MR protocol included structural imaging as well as diffusion tensor imaging (DTI). With the RARE (Rapid Acquisition with Relaxation Enhancement) sequence, T2-weighted (T2w) images were acquired in the coronal plane centered 5 mm caudal of the posterior edge of the olfactory bulb (repetition time/echo time (TR/TE) 4000/65 ms, field of view (FOV) of 3.7 cm x 3.7 cm, slice thickness 2 mm, slice gap 0.1 mm, contiguous slices 12, matrix 256 × 128, and number of averages 5).

The DTI-EPI sequence was used to acquire diffusion weighted images with the same geometrical parameters as anatomic images but with a smaller matrix size (128 × 128, slice thickness 1 mm, TR/TE 4000/23 ms, diffusion directions 30, with 3 diffusion per direction, four segments, one average, d/D = 5/10 ms, gradient duration 2.18 ms, and four b values of 0, 125, 985 and 1925s/mm² respectively.

All the data were pre-processed using custom software written in MATLAB (Mathworks, Natick, MA). DTI data were post-processed with the following bi-exponential intravoxel incoherent motion (IVIM) model [37],

$$\frac{S(b)}{S(0)} = fe^{-b(D+D^*)} + (1-f)e^{-bD}$$

In this equation *f* is the perfusion fraction, *D* is diffusion parameter and *D** is the pseudo-diffusion parameter. For calculating maps of each of these parameters, we used MATLAB optimization toolbox (Mathworks, Natick, MA).

2.9.1. Statistical analysis

Quantitative data obtained from these investigations were analyzed using “R” platform (version 3.5.3, R Development Core Team 2020). Parametric statistical comparisons between the data sets were made based on the representation of mean ± standard deviation (SD) unless otherwise stated. Student’s *t*-test (parametric data) was used for statistical analyses. Statistical analyses between groups were performed using two-way repeated measurements, analysis of variance (ANOVA) with TukeyHSC post hoc tests for multiple comparisons. A *P*-value < 0.05 was considered significant.

3. Results

High-sodium diet regimen did not increase the MAP of APP/PS1 mice. A three-month high-sodium diet regimen did not change the MAP of APP/PS1. More specifically, we did not observe statistically significant changes in both the systolic and diastolic blood pressure of APP/PS1 because of the high-sodium diet. However, the same diet increased the MAP of WTC when compared to the low-sodium-fed WTC (*p* = 0.0002). This diet significantly increased the diastolic blood pressure of WTC compared to the low-sodium-fed group (*p* = 0.001). Moreover, the difference between APP/PS1 and WTC MAP after a high-sodium diet regimen was significant (*p*<0.0001). Systolic and diastolic blood

Table 1
Mouse systolic/diastolic blood pressure (mm Hg).

Experimental Groups	Low-sodium diet (systolic / diastolic)	High-sodium diet (systolic/diastolic)
WTC	134.0 ± 2.8 / 114.75 ± 5.0	162.1 ± 3.8 / 137.75 ± 2.6
APP/PS1	120.0 ± 7.8 / 93.67 ± 5.6	121.0 ± 4.6 / 92.67 ± 2.9

WTC: wild-type controls; APP/PS1: beta-amyloid precursor protein (APPswe), and a mutant human presenilin-1 (PS1). Data are presented as mean ± SD (*n* = 10).

pressure data are summarized in Table 1.

A high-sodium diet regimen causes the death of hippocampal pyramidal cells. Only a small number of hippocampal pyramidal cells shrank with condensed and deeply stained nuclear chromatin in the APP/PS1 group fed a low-sodium diet (Fig. 2D and E upper panel). On the other hand, in the APP/PS1 group that fed a high-sodium diet, we observed that the majority of hippocampal neurons exhibited pyknosis and deep staining (Fig. 2D and E lower panel). Representative photomicrographs show Nissl staining in CA1 region of mouse hippocampus in the two groups ($\times 200$). We found a statistically significant increase in damage cells in both hippocampal and cortical areas of APP/PS1 fed high-sodium diet compared to APP/PS1 fed low-sodium diet ($p < 0.001$, Fig. 2D). **(B and C-upper panel)** In APP/PS1 and WTC group with a LS diet, only a small number of hippocampal pyramidal cells were shrunken with condensed and deeply stained nuclear chromatin (dark blue). **(B and C-lower panel)** In APP/PS1 and WTC group with a HS diet regimen, more hippocampal neurons exhibited pyknosis and deep staining (dark blue). **(D)** In this panel the bar plots represents number of damaged cells (mean + SD) in ROIs of cortex. There are significant differences in the number of damaged cells identified by Nissl staining between LS and HS fed APP/PS1 groups in both cortical and hippocampal areas. Statistical results are shown based on mean \pm SD data ($n = 6$, ** $p < 0.01$, *** $p < 0.001$). **(E)** This panel represents the total number of injured cells (mean + SD) in ROIs of the hippocampal region.

Similar to the cortex, there are significant differences between the number of damaged cells identified by Nissl staining between LS and HS-fed APP/PS1 as well as WTC groups.

High-sodium diet reduces cerebral vessel density in the cortex and hippocampus. Fig. 3B shows representative microphotographs of cortical and hippocampal areas of mouse brain from the low-sodium diet group stained with collagen IV. Fig. 3B shows representative microphotographs of cortical and hippocampal areas of APP/PS1 mouse brain from the high-sodium diet group. The comparison between these two figures indicates that cerebrovascular density is reduced in high-sodium diet APP/PS1. Fig. 3D summarizes statistical comparison between cerebrovascular density, as defined by number of collagen IV stained vessel segments per frame, in both cortex and hippocampus of two experimental groups ($n = 12$, ** $p < 0.01$, * $p < 0.05$). Fig. 3A represents anatomical areas in coronal sections (Cortex and Hippocampus) where samples were chosen for vessel counting and comparison.

A high-sodium diet regimen alters cerebrovascular morphology in the APP/PS1 mouse model of AD. A high-sodium diet for three months thickens cerebral vessels in the APP/PS1 group. Microphotographs of the cortical regions of mouse brain from WTC fed low-sodium diet, APP/PS1 group fed low-sodium diet, and APP/PS1 mouse fed high-sodium diet are shown in Fig. 4A. It is evident from this panel (Panel A) that vessels in the APP/PS1 fed a high-sodium diet are thicker. Statistical comparison shows a significant increase in cerebral vessel diameters in

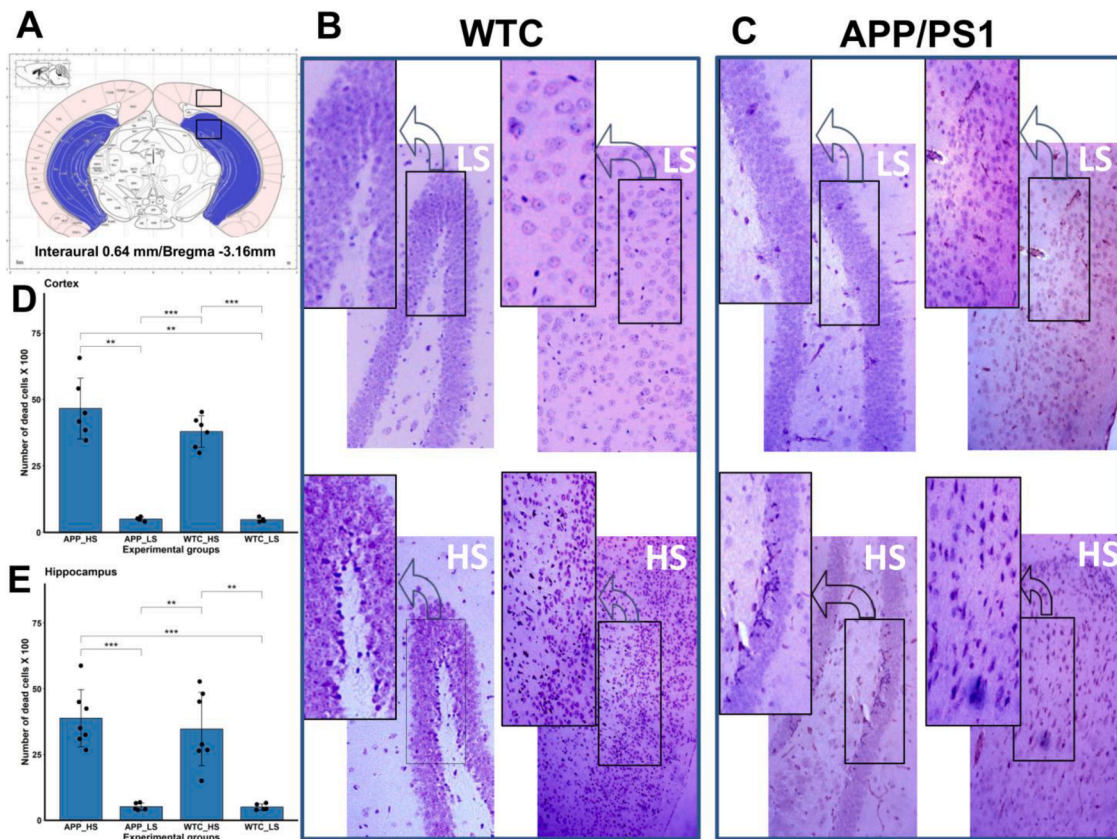


Fig. 2. A high-sodium diet regimen impacts hippocampal and cortical pyramidal cells. (A) Schematic illustration of regions in coronal sections that were selected for neuronal cell counting in the hippocampus and cerebral cortex respectively. Nissl-stained dark neurons are seen in the CA1 region of mouse hippocampus and cerebral cortex in the four experimental groups, high sodium diet (HS) and low sodium diet (LS), the APP/PS1 groups, and controls ($\times 200$). **(B and C-upper panel)** In the APP/PS1 and WTC group with a LS diet, only a small number of hippocampal pyramidal cells were shrunken with condensed and deeply stained nuclear chromatin (deep blue). **(B and C-lower panel)** In the APP/PS1 and WTC group with a HS diet regimen, more hippocampal neurons exhibited pyknosis and deep staining (dark blue). **(D)** In this panel, the bar plots represent the number of injured cells (mean + SD) in ROIs of cortex. There are significant differences in the number of damaged cells identified by Nissl staining between LS and HS fed APP/PS1 groups in both cortical and hippocampus areas. **(E)** The bar plots illustrate the number of injured cells (mean + SD) within ROIs in the hippocampal region. Similar to the cortex, there are significant differences between the number of damaged cells identified by Nissl staining between LS and HS-fed APP/PS1 as well as WTC groups. The difference between HS fed groups and LS fed groups is statistically significant. Statistical results are shown based on mean \pm SD data ($n = 6-7$, ** $p < 0.01$, *** $p < 0.001$).

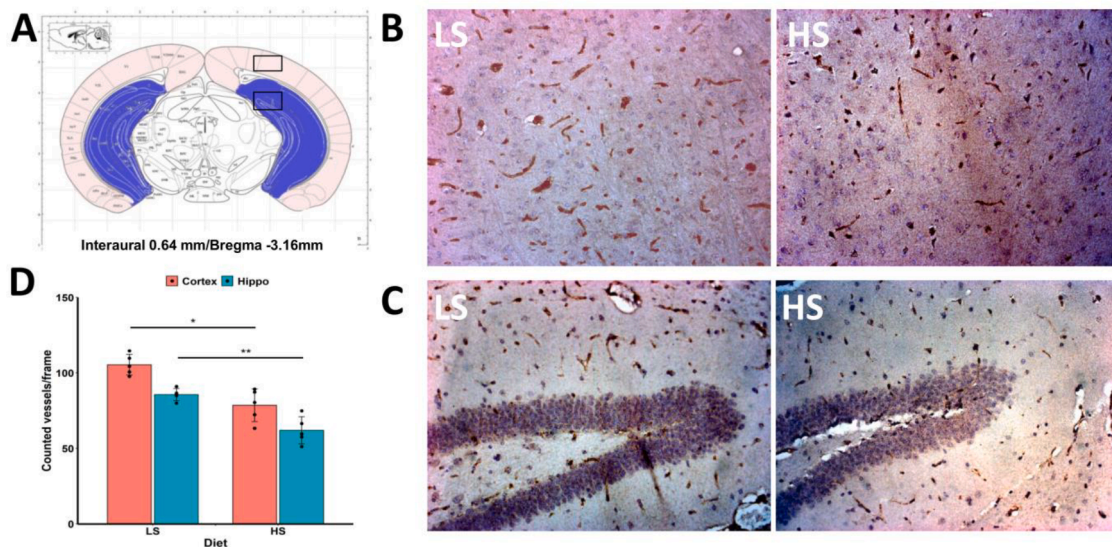


Fig. 3. The density of collagen-stained vessels in the APP/PS1 high-sodium diet fed group is less than in the low-sodium diet fed group. (A) Representation of anatomical area where cortical (top box) and hippocampal (bottom box) samples were chosen for vessel counting. (B) A representative microphotograph of mouse brain cortex from the low-sodium diet (LS) and high-sodium diet (HS) groups. (C) A representative microphotograph of mouse brain hippocampus from LS and HS groups. Both panels show that the cerebrovascular density is lower in the HS group than in the LS group. (D) Statistical comparison between cerebrovascular density in both cortex and hippocampus of two experimental groups, as defined by the number of collagen IV stained vessel segments per frame, are represented in this panel. Results are presented as mean ± SD ($n = 6$, $**p < 0.01$, $*p < 0.05$). Collagen IV stained vessels are shown in dark brown.

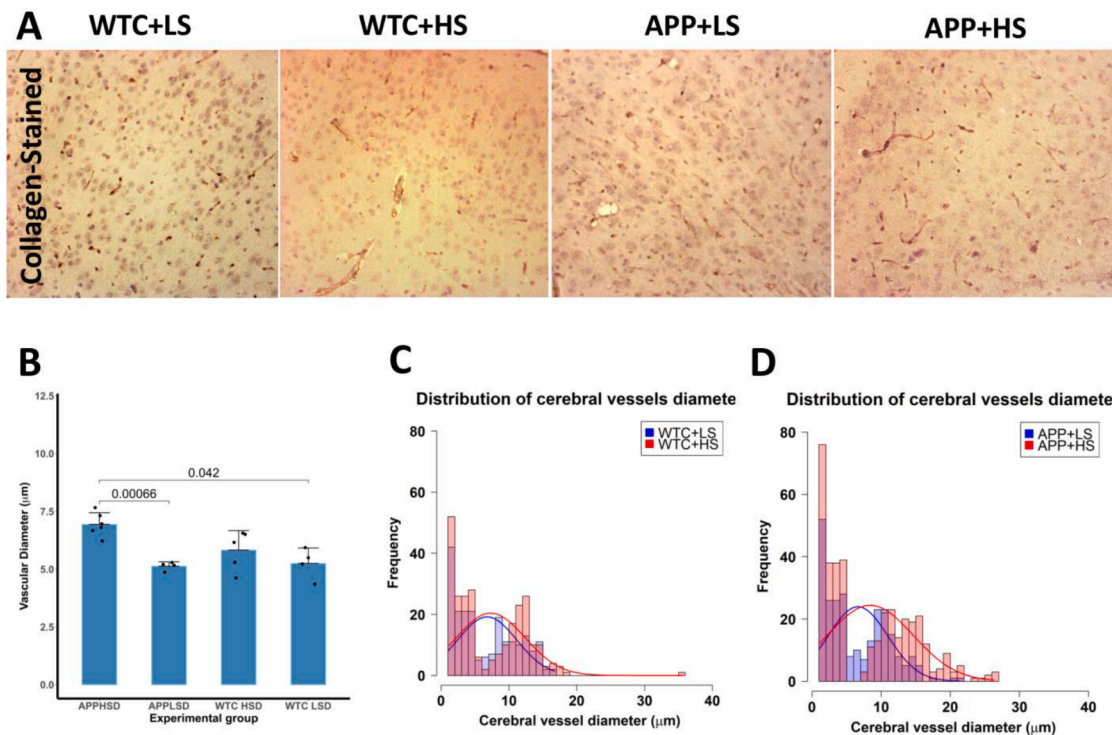


Fig. 4. The impact of a high-sodium diet regimen on vascular morphology in the presence of Aβ. A 3-month high-sodium diet regimen increased vessel diameter in APP/PS1 compared to wild-type controls (WTC). Vascular morphological changes were analyzed by collagen IV staining. (A) This panel shows representative microphotographs of collagen IV stained coronal sections (5 μm) within the coordinates of 2.46 mm interaural and -1.34 mm bregma and 0.64 mm interaural and -3.16 mm bregma from all experimental groups. (B) Statistical comparison of vascular thickness in cortical areas stained by collagen IV is shown in this panel. Vascular diameter lines were drawn perpendicular to the longitudinal axis in the center of the stained vessel. Measured data per frame were statistically analyzed for mean and standard deviation in each frame in cortical areas for all experimental groups. (C) The distribution of cerebral vessel thickness in two groups of WTC. One group was fed a low-sodium diet, and another group was fed a high-sodium diet. (D) The distribution of cerebral vessel thickness in two groups of APP/PS1. One group was fed a low-sodium diet, and another one was fed a high-sodium diet. Results in panel B are presented as mean ± SD ($n = 4-6$).

the APP/PS1 high-sodium diet (B). Panels (C) and (D) compare the distribution of cerebral vessels diameter between WTC and APP/PS1 given different diets. As it is clear from plots C and D, a high-sodium diet increases the vessels diameter in the APP/PS1 more than in WTC. Measured data per frame were statistically analyzed for mean and standard deviation in each frame, in cortical areas for all experimental groups. The anatomical areas were the same as used for vascular density analysis indicated in Fig. 3.

After three months of high-sodium diet, cerebral perfusion fraction f increased in WTC but not significantly in APP/PS1 models. We observed that a high-sodium diet regimen increased cerebral perfusion fraction, f in anatomical areas critical for memory and cognition compared to WTC group that fed a low-sodium diet ($p = 0.022$). Fig. 5A shows the anatomy of the area selected from cortex and hippocampus for perfusion fraction analysis. Fig. 5B represents statistical comparison of the mean and SD of averaged perfusion fraction in ROI of cortex and hippocampus. We observed a statistically significant increase in f in cortical areas of WTC fed a high-sodium diet ($p = 0.022$), but not in hippocampal areas ($p = 0.34$). Nevertheless, a high-sodium diet regimen did not significantly alter f in both cortical and hippocampal areas of the APP/PS1 group.

A high-sodium diet regimen did not change water diffusion parameter D in APP/PS1 mouse brain area relevant to memory and cognition. We investigated the integrity and directional diffusions of cortical and hippocampal areas of both APP/PS1 and WTC for the impact of a high-sodium diet. We did not observe any statistically significant differences between D of mice under a high-sodium diet regimen and mice fed a low-sodium diet (Fig. 5C) in both cortical and hippocampal areas. Data are shown as mean \pm SD ($n = 10$).

4. Discussion

In the present study, we found that a 3-month high-sodium diet regimen (4% NaCl) reduced cerebrovascular density while increasing vascular diameters in the APP/PS1 model. A high-sodium diet pronouncedly impacts hippocampal pyramidal cells of APP/PS1. In spite of these changes in cerebrovascular morphology, we did not observe any significant MRI-visible changes in cerebral perfusion and diffusion. Rather than using pharmacological agents in this study, we induced hypertension through diet. Specifically, this study examined the impact of human lifestyle diets leading to hypertension on the development of AD. We observed that a high-sodium diet regimen significantly increased the MAP of WTC, which was in agreement with the findings from previous studies [34,38]. The results of these studies indicate that a high-sodium diet regimen may alter the cerebrovascular structure of APP/PS1 in a different way than WTC.

A high-sodium diet regimen implemented in this study resulted in a high MAP in WTC. As such, this model has the potential to be used as an experimental model to investigate the impact of dietary salt loading on diseases such as AD. Our data indicate that in APP/PS1 that fed a low-sodium diet, only a small number of hippocampal pyramidal cells were shrunken (with condensed and deeply stained nuclear chromatin). While, in APP/PS1 with a 3-month high-sodium diet regimen, the majority of hippocampal neurons exhibited pyknosis and deep staining (Fig. 2). Pyramidal neurons are excitatory neurons found in the cortex, hippocampus, and amygdala. Mechanistically a high-sodium diet regimen has been shown to increase ROS in the hippocampus and cause memory loss [28]. However, our data show that the loss of pyramidal cells is accelerated in APP/PS1. It remains to be investigated if the excess production of $A\beta$ exacerbates the impact of a high-sodium diet on

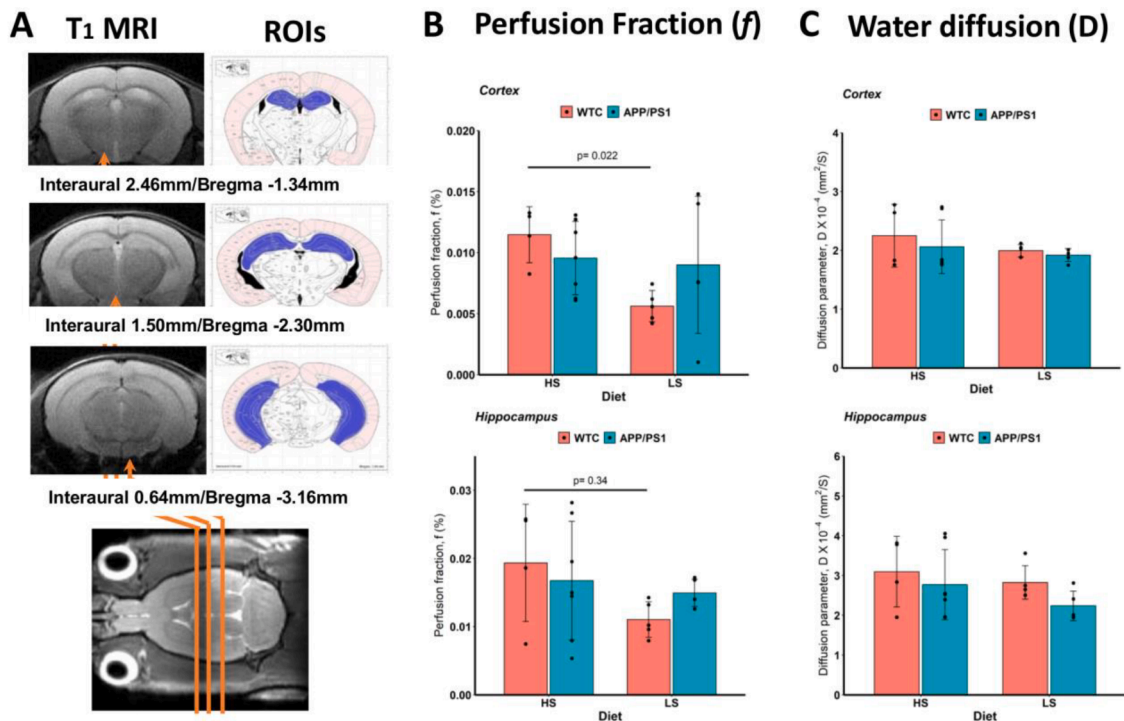


Fig. 5. Cerebral perfusion and diffusion are not changed significantly because of a high-sodium diet regimen in the APP/PS1. A) Illustration of selected regions of interest (ROI) in the coronal views. Cortical (in light pink color) and hippocampal areas (in blue color) in three consecutive slices were analyzed for change in water perfusion and diffusion parameters. B) Four experimental groups including two APP/PS1 mice and two WTC groups were used to analyze perfusion data (one of each was fed a high-sodium diet while another one was fed a low-sodium diet). Two key parameters of the intravoxel incoherent motion (IVIM) model, namely f (the perfusion fraction), and D (the diffusion parameter) were compared between these experimental groups. Na⁺ loading significantly increased the CBF in cortical areas but not in the hippocampus area of WTC. On the other hand, there was no significant difference between the f of APP/PS1 mice fed a low-sodium diet and APP/PS1 mice fed a high-sodium diet ($n = 5-7$). C) This panel shows the effect of a high-sodium diet regimen on water diffusion D in the cortical and hippocampal area of APP/PS1 mice and controls. Data are presented as mean \pm SD ($n = 5-7$). As it is apparent from this figure, we did not observe any statistically significant differences between the D of mice on a high-sodium diet regimen and mice fed a low-sodium diet.

pyramidal neurons.

We observed that in APP/PS1 models, dietary salt loading decreased the number of collagen IV stained cerebral vessels in cortical and hippocampal areas. High-sodium diets have been implicated in cerebral vessel damage because of induced hypertension [39,40]. However, recent findings indicate a direct relationship between dietary salt loading and cerebrovascular remodeling, as well as cognitive impairment [39,41]. In humans, a short-term regimen of a high-sodium diet (14.7 g/day for seven days) has been associated with impaired microvascular reactivity regardless of changes in MAP, body composition, or fluid status [27]. Others further pushed the same line of research to show that a high-sodium diet suppresses endothelial function [25,26]. Mechanistically the suppression of nitric oxide [23,42] and ROS activation because of a high-sodium diet were connected to impaired endothelial functions [24].

Collagen IV fibers coat the lumens of all vessels. In blood vessels larger than the arteriole or venule, additional collagen IV fibers represent the basement membranes of medial smooth muscles. By immunohistochemical staining of collagen IV, it is possible to identify the basement membrane on blood vessels. It is therefore not possible to distinguish between an enlarged basement membrane and an enlarged vessel by using collagen IV staining alone. We conducted this study solely in order to determine the diameter and distribution of cerebral vessels. We did not expect to observe a sole enlargement of the basement membrane in the present experiment setting. In this regard, collagen IV stains may be associated with the diameter of the vessels. The vascular anatomy can, however, be better understood by staining multiple vessels at the same time.

We observed that dietary salt loading caused cerebral vessels to become thicker in both hippocampal and cortical areas of APP/PS1 models (by analyzing collagen IV stained tissues). The impact of diet and disease on cerebral vessels has been studied in different models of diseases. For example, morphological and architectural changes of cerebral vessels have been correlated with CBF alteration in the APP23 transgenic mice model of AD [43]. Previous studies also reported that chronic high MAP causes structural alteration of cerebral vessels [44]. To compare our results with results obtained from other rodent models of diseases, we have to consider that there is variation in cerebral vessel diameter as a function of strain [45].

Physiological deficits associated with AD include reduced CBF (cerebral hypoperfusion). [43]. In this study, we investigated the effects of a high-sodium regimen on CBF in an AD model. We did not observe a statistically significant difference between the CBF of APP/PS1 and WTC fed a low-sodium diet. On the other hand, a high-sodium diet regimen caused a statistically significant increase in CBF in WTC but not in the APP/PS1 group. Although our data show a slight reduction in APP/PS1 CBF in high-sodium diet groups, it was not statistically significant compared to WTC littermates. Mounting et al. also found that the CBF was preserved in a model of cerebral microvascular amyloidosis by using MRI [44].

The cerebrovascular autoregulation mechanism responds to transient hypoperfusion and hyperperfusion by regulating cerebrovascular reactivity [45]. An impaired autoregulation of cerebral perfusion results in hypoperfusion or hyperperfusion of the brain. A high MAP or AD pathology can impair cerebrovascular reactivity, which negatively impacts the autoregulation mechanism. A study by Allen et al. shows that a high-sodium diet, whether short-term or chronic, impairs cerebrovascular autoregulation [46]. In addition, they demonstrate that salt-induced ANG II suppression initiates impaired CBF regulation [46]. The results of another study on arterial hypertension among the elderly indicate that a decrease in MAP is associated with tau pathology and a decline in memory [47].

Recent studies have shown that hypertension is associated with disrupted white matter integrity in humans [48–50]. In this study, we did not find any evidence that tissue integrity was disrupted in cortical and hippocampal areas of APP/PS1 mice fed high-sodium diets.

Analyzing mean diffusivity (MD) and fractional anisotropy (FA) of acquired diffusion data by DTI [34] and our data acquired by the IVIM model and analyzing D and f do not provide evidence for tissue integrity impairment (visible by MRI) in AD models. It is likely that the limitations of APP/PS1 models are responsible for this discrepancy between animal model data and human data. The APP/PS1 models do not fully represent the underlying pathogenesis of AD. Also, those reported human data were mostly collected from relatively small sample sizes and specific brain regions. However, consistent with our findings, Holland et al. also showed that hypertension has minimal impact on white matter integrity in aged hypertensive rats that were fed a high-fat diet [51].

This study has several limitations. This study aimed to model the impact of a high sodium diet on cerebrovascular morphology and function in AD. However, it is not known if a high-sodium diet has the same impact on rodents' physiology as on humans. Although we induced hypertension in an animal model with a high-sodium diet regimen in order to simulate human hypertension, we did not distinguish between salt-sensitive and salt-insensitive mice in this experiment. As a matter of fact, this is the case for humans as well. For this study to be applicable to humans, it is crucial to distinguish between salt-sensitive and salt-insensitive individuals.

The APP/PS1 was used in this study, as is the case with most AD studies involving animal models. The APP/PS1 exhibits remarkable elevation of β -amyloid production associated with certain behavioral abnormalities. In the cortex and hippocampus of APP/PS1 mice, vessels were observed to be thinner, disorganized, and less uniform [32]. As a result of a high-sodium diet, this vascular morphology was altered in this study. Nevertheless, further research is necessary to understand the mechanism of APP/PS1 vascular changes and the influence of genetic modifications on salt sensing and hypertension. Despite all of these limitations, we consider our study to be one of the few studies that link cerebrovascular morphology and AD. However, the data we have collected indicate that high-sodium diets affect cerebrovascular morphology and cerebral perfusion differently in APP/PS1 than in WTC.

Hypertension is most often associated with the direct relationship between high sodium diets and brain function. In this study, we present data regarding the effects of high-sodium diets on cerebrovascular morphology without resulting in significant MAP increases in APP/PS1 models. Our findings suggest that dietary salt loading may have a direct impact on cerebrovascular morphology and function in the APP/PS1.

Declaration of Competing Interest

The authors declare no conflict of interest.

Acknowledgments

The authors gratefully acknowledge financial support from the Alzheimer's Association (NIRG-12-242467) and Florida Department of Health (20A18).

References

- [1] T.T. van Sloten, A.D. Protogerou, R.M. Henry, M.T. Schram, L.J. Launer, C. D. Stehouwer, Association between arterial stiffness, cerebral small vessel disease and cognitive impairment: a systematic review and meta-analysis, *Neurosci. Biobehav. Rev.* 53 (2015) 121–130.
- [2] D.A. Nation, C.E. Wierenga, L.R. Clark, S.I. Dev, N.H. Stricker, A.J. Jak, D. P. Salmon, L. Delano-Wood, K.J. Bangen, R.A. Rissman, T.T. Liu, M.W. Bondi, Cortical and subcortical cerebrovascular resistance index in mild cognitive impairment and Alzheimer's disease, *J. Alzheimers Dis.* 36 (2013) 689–698.
- [3] L. Ostergaard, R. Aamand, E. Gutierrez-Jimenez, Y.C. Ho, J.U. Blicher, S. M. Madsen, K. Nagenthiraja, R.B. Dalby, K.R. Drasbek, A. Moller, H. Braendgaard, K. Mouridsen, S.N. Jespersen, M.S. Jensen, M.J. West, The capillary dysfunction hypothesis of Alzheimer's disease, *Neurobiol. Aging* 34 (2013) 1018–1031.
- [4] K.E. Biron, D.L. Dickstein, R. Gopaul, W.A. Jefferies, Amyloid triggers extensive cerebral angiogenesis causing blood brain barrier permeability and hypervascularity in Alzheimer's disease, *PLoS One* 6 (2011) e23789.
- [5] R.E. Bennett, A.B. Robbins, M. Hu, X. Cao, R.A. Betensky, T. Clark, S. Das, B. T. Hyman, Tau induces blood vessel abnormalities and angiogenesis-related gene

- expression in P301L transgenic mice and human Alzheimer's disease, *Proc. Natl. Acad. Sci. U. S. A.* 115 (2018) E1289–E1298.
- [6] S. Nag, D.W. Kilty, Cerebrovascular changes in chronic hypertension. Protective effects of enalapril in rats, *Stroke* 28 (1997) 1028–1034.
- [7] D.I. Barry, Cerebral blood flow in hypertension, *J. Cardiovasc. Pharmacol.* 7 (Suppl 2) (1985) S94–S98.
- [8] M. Muller, Y. van der Graaf, F.L. Visseren, W.P. Mali, M.I. Geerlings, S.S. Group, Hypertension and longitudinal changes in cerebral blood flow: the SMART-MR study, *Ann. Neurol.* 71 (2012) 825–833.
- [9] G. Reed, M. Devous, Cerebral blood flow autoregulation and hypertension, *Am. J. Med. Sci.* 289 (1985) 37–44.
- [10] M. Wiesmann, C. Capone, V. Zerbi, L. Mellendijk, A. Heerschap, J.A. Claassen, A. J. Kiliaan, Hypertension impairs cerebral blood flow in a mouse model for Alzheimer's disease, *Curr. Alzheimer Res.* 12 (2015) 914–922.
- [11] A.M. Brickman, V.A. Guzman, M. Gonzalez-Castellon, Q. Razlighi, Y. Gu, A. Narkhede, S. Janicki, M. Ichise, Y. Stern, J.J. Manly, N. Schupf, R.S. Marshall, Cerebral autoregulation, beta amyloid, and white matter hyperintensities are interrelated, *Neurosci. Lett.* 592 (2015) 54–58.
- [12] T. Thomas, G. Thomas, C. McLendon, T. Sutton, M. Mullan, beta-Amyloid-mediated vasoactivity and vascular endothelial damage, *Nature* 380 (1996) 168–171.
- [13] M.P. Murphy, R.A. Corriveau, D.M. Wilcock, Vascular contributions to cognitive impairment and dementia (VCID), *Biochim. Biophys. Acta* 1862 (2016) 857–859.
- [14] C.B. Wright, A. Flores, Vascular contributions to cognitive impairment, *Neurol. Pract.* 5 (2015) 201–208.
- [15] R. Goel, S.A. Bhat, N. Rajasekar, K. Hanif, C. Nath, R. Shukla, Hypertension exacerbates predisposition to neurodegeneration and memory impairment in the presence of a neuroinflammatory stimulus: protection by angiotensin converting enzyme inhibition, *Pharmacol. Biochem. Behav.* 133 (2015) 132–145.
- [16] A. Kruyer, N. Soplop, S. Strickland, E.H. Norris, Chronic hypertension leads to neurodegeneration in the TgSwDI mouse model of Alzheimer's disease, *Hypertension* 66 (2015) 175–182.
- [17] V.H. Perry, C. Holmes, Microglial priming in neurodegenerative disease, *Nat. Rev. Neurol.* 10 (2014) 217–224.
- [18] A. Csiszar, Z. Tucek, P. Toth, D. Sosnowska, T. Gautam, A. Koller, F. Deak, W. E. Sonntag, Z. Ungvari, Synergistic effects of hypertension and aging on cognitive function and hippocampal expression of genes involved in beta-amyloid generation and Alzheimer's disease, *Am. J. Physiol. Heart Circ. Physiol.* 305 (2013) H1120–H1130.
- [19] Z. Sun, Aging, arterial stiffness, and hypertension, *Hypertension* 65 (2015) 252–256.
- [20] C. Catena, G. Colussi, G. Brosolo, F. Martinis, F. Pezzutto, F. Nait, L.A. Sechi, 1c.12: dietary salt intake and aldosterone-related organ damage in hypertension, *J. Hypertens.* 33 (Suppl 1) (2015) e12–e13.
- [21] M.P. Blaustein, F.H. Leenen, L. Chen, V.A. Golovina, J.M. Hamlyn, T.L. Pallone, J. W. Van Huysse, J. Zhang, W.G. Wier, How NaCl raises blood pressure: a new paradigm for the pathogenesis of salt-dependent hypertension, *Am. J. Physiol. Heart Circ. Physiol.* 302 (2012) H1031–H1049.
- [22] I. Drenjancevic-Peric, B. Jelakovic, J.H. Lombard, M.P. Kunert, A. Kibel, M. Gros, High-salt diet and hypertension: focus on the renin-angiotensin system, *Kidney Blood Press. Res.* 34 (2011) 1–11.
- [23] M.A. Boegehold, Effect of dietary salt on arteriolar nitric oxide in striated muscle of normotensive rats, *Am. J. Physiol.* 264 (1993) H1810–H1816.
- [24] D.M. Lenda, B.A. Sauls, M.A. Boegehold, Reactive oxygen species may contribute to reduced endothelium-dependent dilation in rats fed high salt, *Am. J. Physiol.-Heart Circulat. Physiol.* 279 (2000) H7–H14.
- [25] C.P. Guo, Z. Wei, F. Huang, M. Qin, X. Li, Y.M. Wang, Q. Wang, J.Z. Wang, R. Liu, B. Zhang, H.L. Li, X.C. Wang, High salt induced hypertension leads to cognitive defect, *Oncotarget* 8 (2017) 95780–95790.
- [26] G. Faraco, D. Brea, L. Garcia-Bonilla, G. Wang, G. Racchumi, H. Chang, I. Buendia, M.M. Santisteban, S.G. Segarral, K. Koizumi, Y. Sugiyama, M. Murphy, H. Voss, J. Anrather, C. Ladeola, Dietary salt promotes neurovascular and cognitive dysfunction through a gut-initiated TH17 response, *Nat. Neurosci.* 21 (2018), 240–+.
- [27] L. Baric, I. Drenjancevic, A. Matic, M. Stupin, L. Kolar, Z. Mihaljevic, H. Lenasi, V. Seric, A. Stupin, Seven-day salt loading impairs microvascular endothelium-dependent vasodilation without changes in blood pressure, body composition and fluid status in healthy young humans, *Kidney Blood Press. Res.* 44 (2019) 835–847.
- [28] Q. Ge, Z. Wang, Y. Wu, Q. Huo, Z. Qian, Z. Tian, W. Ren, X. Zhang, J. Han, High salt diet impairs memory-related synaptic plasticity via increased oxidative stress and suppressed synaptic protein expression, *Mol. Nutr. Food Res.* 61 (2017).
- [29] T. Malm, J. Koistinaho, K. Kanninen, Utilization of APPsw/PS1dE9 transgenic mice in research of Alzheimer's disease: focus on gene therapy and cell-based therapy applications, *Int. J. Alzheimers Dis.* 2011 (2011), 517160.
- [30] K.C. Ahn, C.R. Learman, G.L. Dunbar, P. Maiti, W.C. Jang, H.C. Cha, M.S. Song, Characterization of impaired cerebrovascular structure in APP/PS1 mouse brains, *Neuroscience* 385 (2018) 246–254.
- [31] X. Lu, M. Moeini, B. Li, Y. Lu, R. Damseh, P. Pouliot, E. Thorin, F. Lesage, A pilot study investigating changes in capillary hemodynamics and its modulation by exercise in the APP-PS1 Alzheimer mouse model, *Front. Neurosci.* 13 (2019) 1261.
- [32] J.I. Szu, A. Obenaus, Cerebrovascular phenotypes in mouse models of Alzheimer's disease, *J. Cereb. Blood Flow Metab.* 41 (2021) 1821–1841.
- [33] D.N. Ferreira, I.A. Katayama, I.B. Oliveira, K.T. Rosa, L.N. Furukawa, M.S. Coelho, D.E. Casarini, J.C. Heimann, Salt-induced cardiac hypertrophy and interstitial fibrosis are due to a blood pressure-independent mechanism in Wistar rats, *J. Nutr.* 140 (2010) 1742–1751.
- [34] S. Taheri, J. Yu, H. Zhu, M.S. Kindy, High-sodium diet has opposing effects on mean arterial blood pressure and cerebral perfusion in a transgenic mouse model of Alzheimer's disease, *J. Alzheimers Dis.* 54 (2016) 1061–1072.
- [35] S.E. Thatcher, *The Renin-Angiotensin-Aldosterone system: Methods and Protocols*, Humana Press: Springer, New York, NY, 2017.
- [36] M.J. Fischer, S. Uchida, K. Messlinger, Measurement of meningeal blood vessel diameter *in vivo* with a plug-in for ImageJ, *Microvasc. Res.* 80 (2010) 258–266.
- [37] D. Le Bihan, What can we see with IVIM MRI? *Neuroimage* 187 (2019) 56–67.
- [38] A. Walkowska, M. Kuczeriszka, J. Sadowski, K.H. Olszynski, L. Dobrowolski, L. Cervenka, B.D. Hammock, E. Kompanowska-Jezierska, High salt intake increases blood pressure in normal rats: putative role of 20-HETE and no evidence on changes in renal vascular reactivity, *Kidney Blood Press. Res.* 40 (2015) 323–334.
- [39] M.M. Santisteban, C. Iadecola, Hypertension, dietary salt and cognitive impairment, *J. Cereb. Blood Flow Metab.* 38 (2018) 2112–2128.
- [40] S. Iida, G.L. Baumbach, J.L. Lavoie, F.M. Faraci, C.D. Sigmund, D.D. Heistad, Spontaneous stroke in a genetic model of hypertension in mice, *Stroke* 36 (2005) 1253–1258.
- [41] H.E. de Wardener, F.J. He, G.A. MacGregor, Plasma sodium and hypertension, *Kidney Int.* 66 (2004) 2454–2466.
- [42] T.R. Nurkiewicz, M.A. Boegehold, Limitation of arteriolar myogenic activity by local nitric oxide: segment-specific effect of dietary salt, *Am. J. Physiol.* 277 (1999) H1946–H1955.
- [43] C.C. Hays, Z.Z. Zlatar, C.E. Wierenga, The utility of cerebral blood flow as a biomarker of preclinical Alzheimer's disease, *Cell. Mol. Neurobiol.* 36 (2016) 167–179.
- [44] L.P. Munting, M. Derieppe, E. Suidgeest, L. Hirschler, M.J. van Osch, B. Denis de Senneville, L. van der Weerd, Cerebral blood flow and cerebrovascular reactivity are preserved in a mouse model of cerebral microvascular amyloidosis, *Elife* 10 (2021).
- [45] Y.C. Tzeng, C.K. Willie, G. Atkinson, S.J. Lucas, A. Wong, P.N. Ainslie, Cerebrovascular regulation during transient hypotension and hypertension in humans, *Hypertension* 56 (2010) 268–273.
- [46] L.A. Allen, J.R. Schmidt, C.T. Thompson, B.E. Carlson, D.A. Beard, J.H. Lombard, High salt diet impairs cerebral blood flow regulation via salt-induced angiotensin II suppression, *Microcirculation* 26 (2019) e12518.
- [47] L. Glodzki, H. Rusinek, E. Pirraglia, P. McHugh, W. Tsui, S. Williams, M. Cummings, Y. Li, K. Rich, C. Randall, L. Mosconi, R. Osorio, J. Murray, H. Zetterberg, K. Blennow, M. de Leon, Blood pressure decrease correlates with tau pathology and memory decline in hypertensive elderly, *Neurobiol. Aging* 35 (2014) 64–71.
- [48] D.H. Salat, V.J. Williams, E.C. Leritz, D.M. Schnyer, J.L. Rudolph, L.A. Lipsitz, R. E. McGlinchey, W.P. Milberg, Inter-individual variation in blood pressure is associated with regional white matter integrity in generally healthy older adults, *Neuroimage* 59 (2012) 181–192.
- [49] P. Maillard, S. Seshadri, A. Beiser, J.J. Himali, R. Au, E. Fletcher, O. Carmichael, P. A. Wolf, C. DeCarli, Effects of systolic blood pressure on white-matter integrity in young adults in the Framingham Heart Study: a cross-sectional study, *Lancet Neurol.* 11 (2012) 1039–1047.
- [50] C. Rosano, K.Z. Abebe, H.J. Aizenstein, R. Boudreau, J.R. Jennings, V. Venkatraman, T.B. Harris, K. Yaffe, S. Satterfield, A.B. Newman, A.B.C.S. Health, Longitudinal systolic blood pressure characteristics and integrity of white matter tracts in a cohort of very old black and white adults, *Am. J. Hypertens.* 28 (2015) 326–334.
- [51] P.R. Holland, M.A. Pannozzo, M.E. Bastin, A.D. McNeilly, K.J. Ferguson, S. Caughey, M.A. Jansen, G.D. Merrifield, I. Marshall, J.J. Mullins, J.M. Wardlaw, C. Sutherland, K. Horsburgh, Hypertension fails to disrupt white matter integrity in young or aged Fisher (F44) Cyp11a1Ren2 transgenic rats, *J. Cereb. Blood Flow Metab.* 35 (2015) 188–192.